Lyle, M., Koizumi, I., Richter, C., and Moore, T.C., Jr. (Eds.), 2000
Proceedings of the Ocean Drilling Program, Scientific Results, Vol. 167

28. THE BRUNHES–MATUYAMA AND UPPER JARAMILLO TRANSITIONS RECORDED IN SEDIMENTS FROM THE CALIFORNIA MARGIN[1]

Franz Heider,[2,3] Felix Hufenbecher,[2] Ulrike Draeger,[2,4] and Akira Hayashida[5]

ABSTRACT

Two records of the Brunhes–Matuyama (B–M) transition and one record of the upper Jaramillo transition were obtained from sediments of Ocean Drilling Program (ODP) Leg 167 along the California margin. The geomagnetic transitions were sampled with u-channels and closely spaced discrete samples. The discrete samples and u-channels from opposite halves of the core give similar virtual geomagnetic pole (VGP) paths for the upper Jaramillo reversal at Site 1020 (Gorda Ridge). For the B–M transition at Site 1020, the discrete samples and u-channels show different VGP paths. At every site, and especially for the B–M transition at Site 1014 (Tanner Basin), the VGP paths do not reach the geographic South and North Poles. The characteristic remanent magnetization is contaminated with a coring-induced overprint that has coercivities that overlap with the coercivities of the primary magnetization. The presence of a drilling remanence leads to shallow reverse and steep normal inclinations. Model calculations simulate the effects of small overprints along the axis of the sediment core or perpendicular to it. The calculations show that significant changes can occur in the transitional VGP positions because of drilling overprints. The coring-induced overprint often cannot be completely removed by alternating-field demagnetization and may give rise to false transitional directions. Other ODP reversal records should be checked for the presence of coring-induced overprints.

INTRODUCTION

Geomagnetic reversals are an intriguing phenomenon of the Earth's magnetic field. Records of geomagnetic polarity transitions from sediments led to the suggestion that the virtual geomagnetic pole (VGP) paths run preferentially along two bands of longitude, across the Americas and the antipode (Laj et al., 1991; Clement, 1991). It was suggested that certain geophysical parameters, such as the regions of higher seismic velocities in the lower mantle, have a significant control over the reversal process (Laj et al., 1991). The significance of the preferred longitudinal bands has been questioned. Langereis et al. (1992) conclude that the preferred VGP paths can arise from smoothing of pre- and post-transitional directions. The statistical significance of preferred longitudinal VGP bands has also been questioned (McFadden et al., 1993).

Paleomagnetic transitional records from lavas for the past ten million years tend to cluster in at least two specific restricted regions (Hoffman, 1992). These zones correlate with the near-radial flux concentrations of today's nondipole field. Prévot and Camps (1993) in contrast suggest that there is no evidence for preferred cluster zones or longitudinally confined VGP paths in the volcanic rock record. Love's (1998) analysis of paleomagnetic lava data contradicts that of Prévot and Camps (1993) and does not find support for the hypothesis of clustering of transitional VGPs (Hoffman, 1992). On the contrary, Love (1998) concludes that volcanic rocks give intermediate VGPs that tend to fall along American and Asian longitudes.

The natural remanent magnetization (NRM) of sediments is complicated because of postdepositional processes, which lead to the acquisition of magnetization over an extended time period. In addition to these difficulties in remanence acquisition, the NRM of cored sediments can be overprinted by a coring-induced magnetization (CIM). Vertical and radial CIMs were observed on sediment cores from several Ocean Drilling Program (ODP) legs. Fuller et al. (1998) measured axial fields from 1 up to 15 mT pointing along the core barrels and radial fields around a few millitesla within the advanced hydraulic piston corer (APC) inner core barrels. The properties of coring-induced magnetization and the acquisition mechanism were reviewed by Fuller et al. (1998). Below, we examine the transitional VGP paths from three reversals recorded in sediments cored off the California margin. Our results illustrate the sensitivity of VGP paths to factors unrelated to the geomagnetic field. In particular for this study and likely for other studies that use deep-sea drill cores, magnetic overprints acquired during drilling operations prove to be difficult to fully remove using standard alternating-field (AF) demagnetization methods. The bias caused by the overprint is significant enough in these cases that the accuracy, and hence the geomagnetic significance, of the positions of the transitional VGPs is questionable.

SITE LOCATION AND SAMPLING

The sediment records of the Brunhes–Matuyama (B–M) transition and the upper Jaramillo were obtained from ODP Leg 167. Site 1014 is located at 32°50′N, 119°60′W, in the Tanner Basin of the California Borderland (Fig. 1). San Diego is ~290 km east of the location. In the upper 120 m below seafloor (mbsf), the sediments consist of clay and nannofossil ooze. The sedimentation rate in this part of the section is around 8 cm/k.y. (Lyle, Koizumi, Richter, et al., 1997). The B–M transition was sampled continuously with 1.5-m-long u-channels (2 × 2 cm^2 in cross section) and with discrete samples at a spacing of 3 cm across the transition. The u-channels were taken from the archive halves and the single samples from the corresponding working halves of the cores at Sites 1014 and 1020.

Hole 1020C is located at 41°00′N, 126°26′W, on the east flank of the Gorda Ridge (Fig. 1). The sediments in the section where the B–M and the upper Jaramillo transition are recorded consist mainly of clay interbedded with nannofossil clay. The B–M and the upper Jaramillo transition at Site 1020 were sampled with u-channels. Discrete samples were taken at high spatial resolution (one sample every 3 cm) from 75.3 to 78.1 mbsf across the B–M reversal and from 93.3 to 95.4

[1]Lyle, M., Koizumi, I., Richter, C., and Moore, T.C., Jr. (Eds.), 2000. *Proc. ODP, Sci. Results,* 167: College Station TX (Ocean Drilling Program).

[2]Institut für Allgemeine und Angewandte Geophysik, Ludwig-Maximilians-Universität, Theresienstr. 41, 80333 München, Federal Republic of Germany.

[3]Present address: Department of Geological Sciences, 240 Wallace Building, University of Manitoba, Winnipeg, MB, R3T 2N2, Canada. Franz_Heider@umanitoba.ca

[4]Present address: Department of Earth Sciences, University of California at Santa Cruz, Santa Cruz CA 95064, USA.

[5]Earth Sciences Laboratory, Faculty of Science, Doshisha University, Kyoto, 602, Japan.

mbsf across the upper Jaramillo reversal. The sedimentation rate at Site 1020 over the sampled interval is again ~8 cm/k.y.

MEASUREMENTS

The measurements of natural remanent magnetization and anhysteretic remanent magnetization (ARM) of the u-channel samples were carried out at the University of California, Davis, with a 2G pass-through cryogenic magnetometer in a shielded room. The u-channels were measured at 1-cm intervals, but because of the response function of the pick-up coils, only every fourth measurement is independent (Weeks et al., 1993). The stepwise AF demagnetization of the NRM was carried out with steps of 5, 10, 15, 20, 25, 30, 40, and 50 mT. After demagnetizing the NRM, an ARM was applied at 100-mT AF with a 0.05-mT bias field followed by stepwise demagnetization at 20, 25, and 30 mT. In addition, the initial susceptibility (χ) was measured. The saturation isothermal remanent magnetization (SIRM) was induced in a 1-T direct field and stepwise AF demagnetized at 20, 25, and 30 mT.

The NRM, ARM, and isothermal remanent magnetization (IRM) of the discrete samples were measured with a 2G cryogenic magnetometer at the paleomagnetic laboratory of the Universität München. The NRM of all single samples was measured and stepwise AF demagnetized up to 40 or 50 mT. Some of the specimens had already been demagnetized on the ship to an AF step of 20 mT. Magnetic susceptibility was measured with a KLY 2 Kappabridge. The ARM was induced in the single samples at 150-mT AF with a 0.05-mT bias field and the SIRM with a 1-T direct field. Both remanences were demagnetized at 20-mT AF. The remanent coercive force (B_{cr}) and the hysteresis loops of 24 samples were measured with a variable field translation balance.

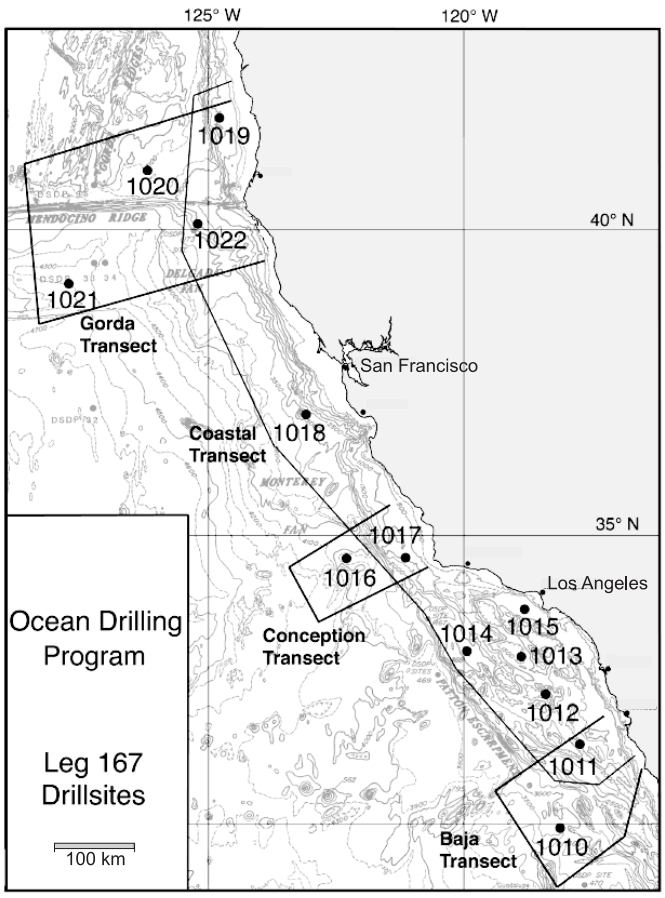

Figure 1. Locations of Sites 1014 and 1020, which were drilled with the advanced hydraulic piston corer during ODP Leg 167 along the California margin.

RESULTS

Natural Remanent Magnetization

The AF demagnetization diagrams (Fig. 2) show in most cases a characteristic remanent magnetization (ChRM) and a steep downward coring-induced overprint for the u-channel measurements. This overprint appears to be removed with alternating fields between 15 and 20 mT. The CIM was not observed in the discrete samples because they had been already demagnetized at 20 mT during Leg 167. Figure 2 shows typical Zijderveld diagrams of samples from Hole 1020C before, during, and after the upper Jaramillo transition. The

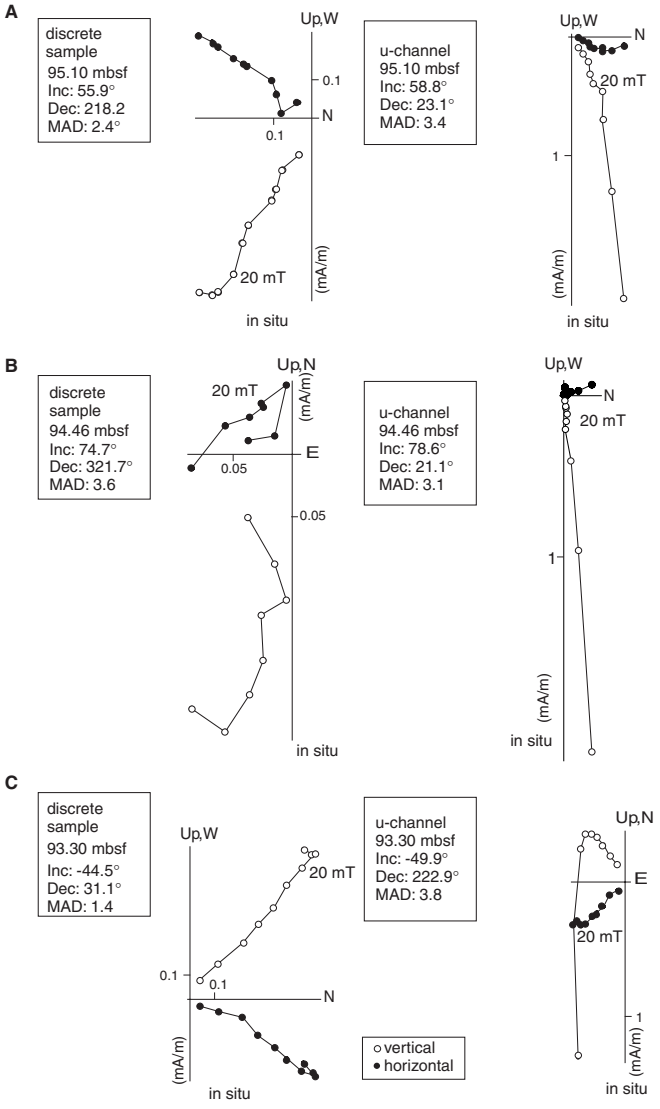

Figure 2. Comparison of representative AF-demagnetization diagrams for samples around the upper Jaramillo transition at Hole 1020C. U-channel measurements (right side) and discrete samples (left side) are from the same depth intervals. MAD is the maximum angle of deviation when fitting a straight line segment to the demagnetization data. (**A**) Directions before the transition, (**B**) transitional directions, and (**C**) directions after the upper Jaramillo reversal. Declinations of u-channels and single samples are different by ~180° because they are from opposite halves of the core.

discrete sample and the u-channel measurements are from the same depth interval before (Fig. 2A), during (Fig. 2B), and after (Fig. 2C) the transition. The ChRMs were obtained by fitting a line through at least four points of the demagnetization diagrams. The inclination values of discrete samples and u-channels are in good agreement. The differences in declination of ~180º occur because u-channel samples were taken from the archive halves and the discrete samples from working halves. The ChRM can be determined quite reliably for samples outside the transition interval, and the principal component analysis is based on at least four demagnetization steps. A minimum of three points were used to fit a line to the AF-demagnetization data for computation of the transitional directions. The directions during a reversal are not as stable as during constant polarity intervals. The maximum angle of deviation for a line fit to the directional data of single samples during the transition is larger than before or after the transition (Fig. 2).

The inclination, corrected declination of the ChRMs, and the normalized NRM for the upper Jaramillo transition at Site 1020 are plotted vs. depth in Figure 3. For the normalized NRM intensities, the demagnetization level of 20 mT is chosen for ARM and NRM. The NRM intensities of single samples from Site 1020 that were measured in the Munich laboratory were 7%–22% higher than the shipboard intensities, which is most likely caused by differences in magnetometer calibration. The ARM values are normalized to the mean value of the investigated depth interval to make single-sample and u-channel results comparable. Normalized values are used because of the difference in amplitude of the alternating field for the acquisition of ARM between the discrete samples and u-channels. The normalized NRM intensities are probably indicators for paleointensity, as demonstrated in the rock magnetism section below. There is good agreement in inclination, declination, and relative paleointensity between discrete samples and the u-channel measurements (open triangles and solid dots, respectively, in Fig. 3). The dashed lines in the plot of inclination represent the values of ±60º expected for an axial geocentric dipole field at the geographic latitude of 41º for Site 1020. The inclinations of the reversed directions are a little shallower than the expected value. This could be the result of a coring-induced overprint that was not completely removed. The normalized relative paleointensity has a minimum at the upper Jaramillo transition. This minimum in relative paleointensity coincides with the jump in declination from 0° to 180°. From the geomagnetic polarity time scale (Cande and Kent, 1995), this depth can be assigned an age of 990 ka. If one employs a constant sedimentation rate of 8 cm/k.y., based on the duration of the Jaramillo Subchron, the length of the transition can be estimated. The directional change for the upper Jaramillo transition takes ~5 k.y. The labeled points in Figure 3 are the ChRM of the discrete samples and u-channel measurements displayed in Figure 2. The low density of data points in the transition region (Fig. 3) is caused by single samples or u-channel intervals that were not interpretable.

The resulting VGP paths of the upper Jaramillo reversal for the u-channel measurements and the single samples are illustrated in Figure 4. The VGPs from the u-channel measurements (solid dots) and the single samples (open triangles) are different. For the u-channels, the VGP path tracks across the Pacific. The only intermediate VGP from a single sample lies near the Gulf of Mexico. Two intermediate VGPs are marked with "1," and the Zijderveld diagrams of the discrete sample and the corresponding u-channel measurement are

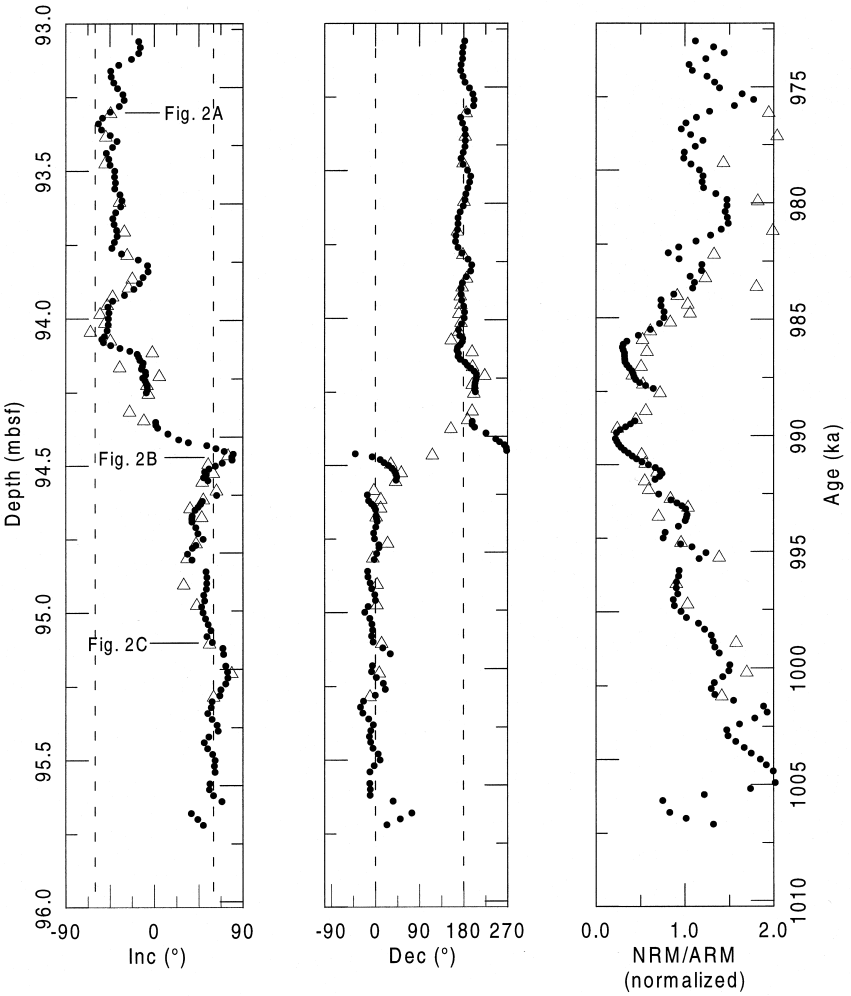

Figure 3. Downhole plot of the characteristic remanence inclination and declination and normalized relative paleointensity of the upper Jaramillo transition from Hole 1020C (Gorda Ridge). Solid dots = the u-channel measurements, open triangles = the results from the discrete samples. The core coordinate system was rotated so that declinations were on average at 0° for normal intervals. Natural remanent magnetization (NRM) and anhysteretic remanent magnetization (ARM) were both AF demagnetized at 20 mT. The age model is based on the ages of the upper Jaramillo (990 ka) and lower Jaramillo (1070 ka) reversals and the assumption of constant sedimentation rate between these two reversals with known depth. The dashed lines represent the values expected for an axial geocentric dipole field.

shown in Figure 2B. The inclinations of these transitional samples are rather steep, so the declination value is not well defined. After removing a large fraction of the CIM with 20-mT AF, the remaining NRM intensities of transitional samples are low (J < 0.2 mA/m). The determination of ChRMs in these intermediate samples is more difficult than for samples from stable polarity intervals.

Figure 5 shows the inclination and declination of the ChRMs and the normalized remanence record vs. depth for the Brunhes–Matuyama transition at Site 1020 (Gorda Ridge). In this record, a precursor to the reversal occurs in the depth interval from 77.35 to 76.90 mbsf.

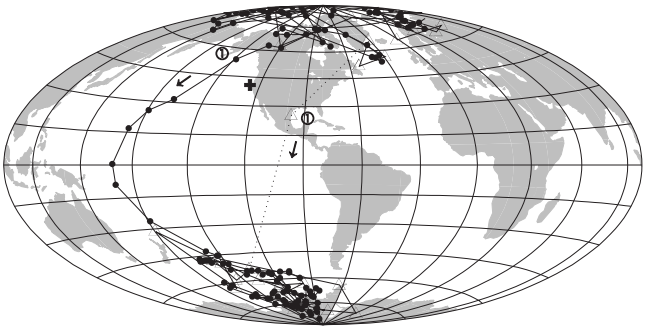

Figure 4. VGP paths for the upper Jaramillo transition at Site 1020 (solid dots = u-channel measurements, open triangles = discrete samples). The only intermediate discrete sample is marked with a "1" as well as the u-channel measurement from the same depth interval. The corresponding Zijderveld diagrams with the AF-demagnetization behavior are shown in Figure 2B.

After a short period of negative inclination, the directional change to normal polarity takes place within 50 cm. With a sedimentation rate of 8 cm/k.y. (Lyle, Koizumi, Richter, et al., 1997), the duration of the directional change corresponds to ~6.2 k.y. An incompletely removed drilling overprint is also seen in this reversal record because the inverse inclinations are considerably shallower than the value expected for a dipole field (dashed lines in Fig. 5).

The VGP path for the B–M transition at Site 1020 is presented in Figure 6A (the results from discrete samples) and in Figure 6B (the u-channel measurements). There is not much similarity between the two VGP paths, but in both cases the VGP jumps several times from normal to reverse polarity and back. For the discrete samples and the u-channel measurements, the VGPs in the Southern Hemisphere do not reach the geographic South Pole. This lack of antipodality can arise from a normal drilling overprint, for example, which leads to shallow negative inclinations.

Magnetic Mineralogy

Several tests have been conducted to identify the main carrier of remanent magnetization at Site 1020. High-coercivity magnetic minerals like hematite are not dominant in this section of the sediments. This is concluded from the $S_{-0.3T}$ parameter (Bloemendal et al., 1992), which is higher than 0.95 for most measurements on u-channels and discrete samples (Fig. 7). In addition, all IRM acquisition curves reach saturation between 200 and 300 mT, which suggests that (titano) magnetite may be present and that high-coercivity minerals are mostly absent. The results of the thermomagnetic curves show no noticeable intensity drop up to 400ºC, and during the heating process,

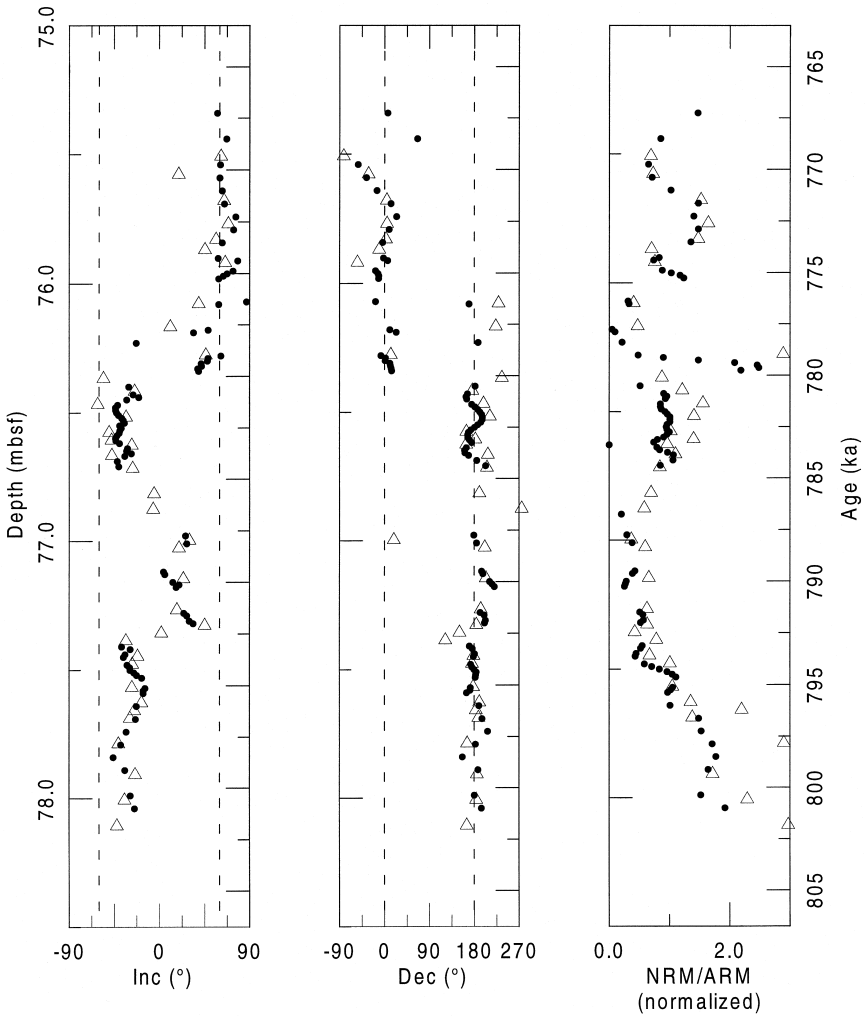

Figure 5. Plot of the characteristic remanent magnetization (inclination and declination) and normalized relative paleointensity vs. depth of the Brunhes–Matuyama transition at Hole 1020C. Solid circles = the u-channel measurements, open triangles = the results of the discrete samples. The agreement between ChRMs from u-channels and discrete samples is good during stable polarity intervals but becomes unsatisfactory during the reversal. Natural remanent magnetization (NRM) and anhysteretic remanent magnetization (ARM) were both AF demagnetized at 20 mT. Age model as in Figure 3. The dashed lines represent the values expected for an axial geocentric dipole field.

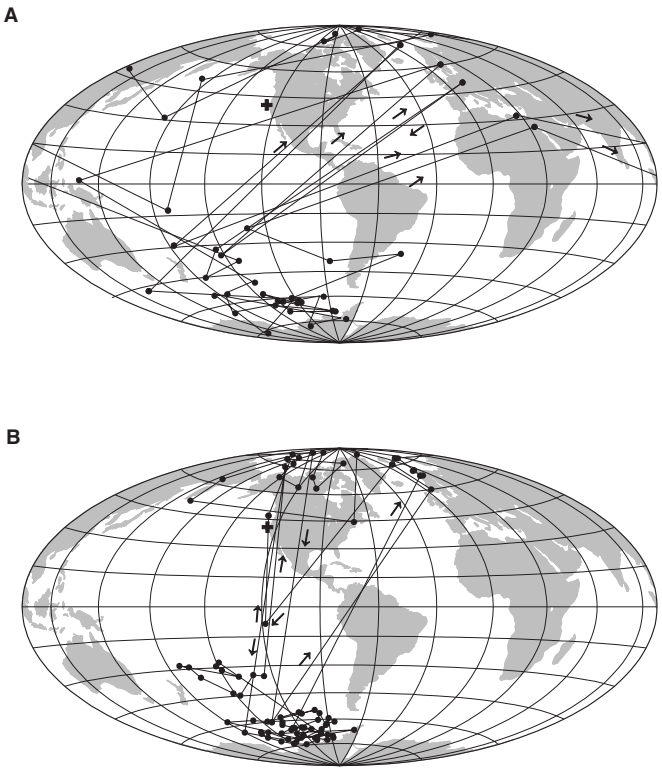

Figure 6. VGP path of the B–M transition from ChRMs of (**A**) discrete samples and (**B**) u-channel measurements from Figure 5. The two types of samples from opposite halves of the core show very different VGPs during the polarity transition.

magnetite is formed around this temperature. It was not possible to demonstrate the presence of primary magnetite with the aid of the thermomagnetic curves because secondary magnetite was formed upon heating.

Downcore variations in magnetic concentration can be estimated from ARM and susceptibility χ. Figure 7 shows the variation of ARM and susceptibility vs. depth. The variations in ARM and χ are less than a factor 5.2 and 2.6, respectively. The concentration of magnetic minerals, therefore, varies much less than a factor of 10, which is one prerequisite for relative paleointensity determination (Tauxe, 1993).

The uniformity of grain size was determined from the hysteresis parameters J_{rs}/J_s and B_{cr}/B_c. The plot of J_{rs}/J_s vs. B_{cr}/B_c (Day et al., 1977) shows that the mean grain size clusters like in many other samples within the pseudo-single-domain range (Fig. 8). The grain sizes of the magnetic particles in the sediments from Hole 1020C (B–M transition and upper Jaramillo) are quite similar, and there are only small variations in magnetic mineralogy across these reversals.

Modeling the Effects of Overprint on the VGP Path

The ChRM from the upper Jaramillo and the B–M transition (Figs. 3, 5) have negative inclinations that are too shallow compared with the value expected at this location for a dipole field. Evidence for a radial overprint comes from the declinations of NRM after 20-mT AF demagnetization of 13 cores of Hole 1020C. Ideally, the declinations should be randomly distributed between 0º and 360º because of the randomly oriented cores. But there is a concentration of samples with high intensities and with declinations clustering around 180º, 270º, or 330º.

Another example of a reversal with a drilling overprint is given in Figure 9 with a record of the B–M transition at Hole 1014D from u-channel measurements. The negative inclinations are again shallow, and the positive inclinations are steep compared with the expected in-

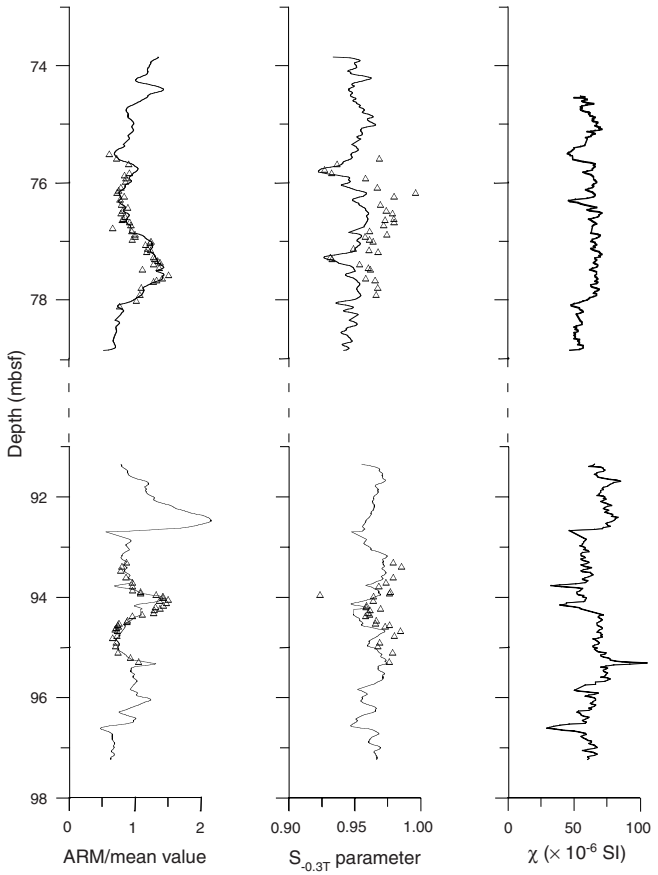

Figure 7. Anhysteretic remanent magnetization (ARM) normalized to its mean value, and $S_{-0.3T}$ parameter and susceptibility from the Brunhes–Matuyama and upper Jaramillo transitions at Hole 1020C.

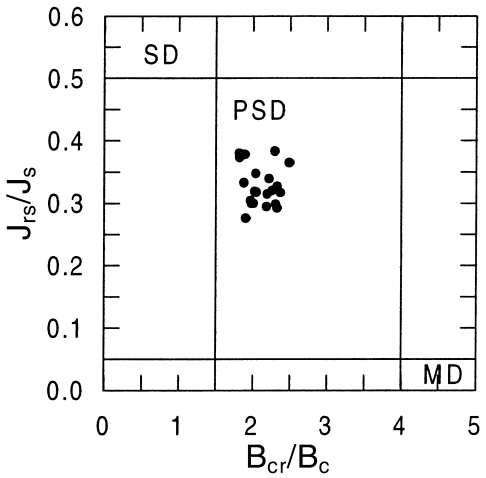

Figure 8. Plot of the hysteresis parameters J_{rs}/J_s vs. B_{cr}/B_c after Day et al. (1977). There is a tight cluster within the pseudo-single-domain (PSD) size range from the B–M and upper Jaramillo transition at Site 1020. Samples are from the two depth intervals shown in Figures 3 and 5. SD = single domain, MD = multidomain.

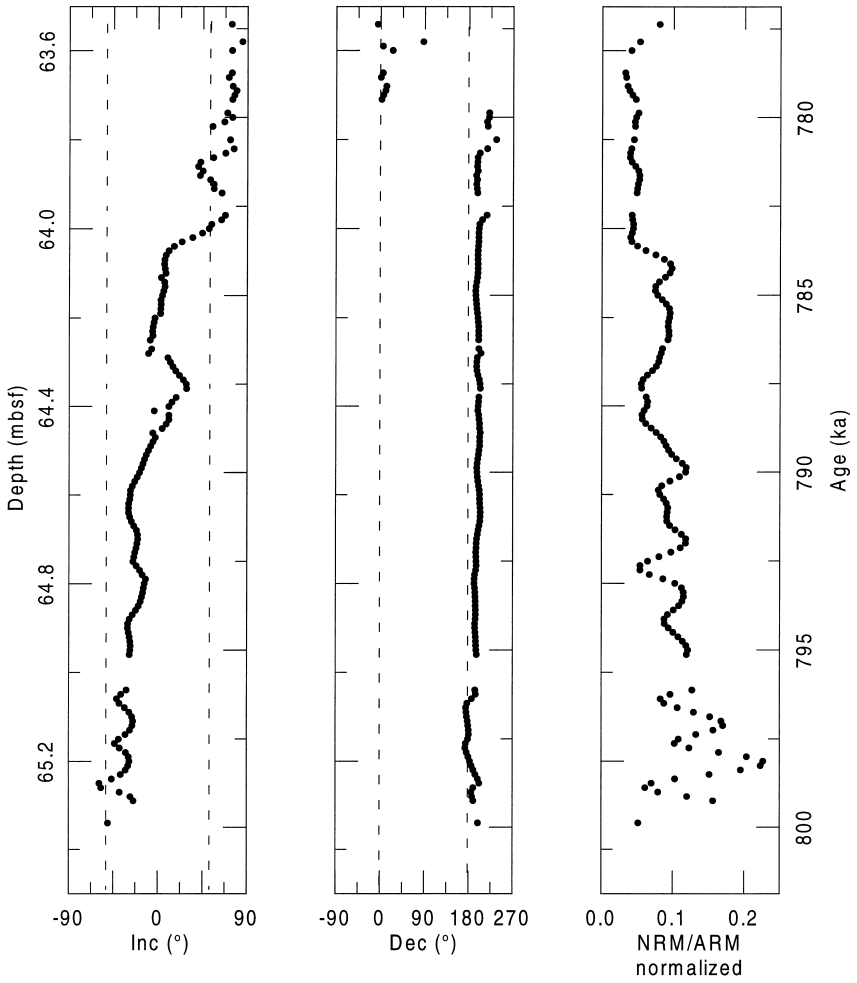

Figure 9. Plot of the characteristic remanent magnetization (inclination and declination) from u-channel measurements and normalized remanence record of the B–M transition at Site 1014. Natural remanent magnetization (NRM) and anhysteretic remanent magnetization (ARM) were both AF demagnetized at 20 mT. The dashed lines represent the values expected for an axial geocentric dipole field.

clination value of 52º at this latitude (dashed lines in Fig. 9). The record from Site 1014 in the Tanner Basin is a good example for the influence of a coring-induced overprint in the positive z-direction. Drilling overprints in various directions were also observed in other ODP cores (Roberts et al., 1996). During the coring process with the APC, the sediments may get an isothermal remanent magnetization overprint in the vertical direction. Another possibility is a radial overprint, which can be acquired by the sediments during the drilling process (Herr et al., 1998; Fuller et al., 1998). The NRM intensity of the sediments from Site 1014 had decreased by about a factor of 30 between the shipboard measurements and the land-based intensity measurements seven months later (F. Heider, J.M. Bock, J.P. Kennett, I. Hendy, J. Matzka, and J. Schneider, unpubl. data). Reorientation of magnetic particles in the expanding sediment is a possible explanation because susceptibility of the sediments remained unchanged between shipboard and land-based measurements. The record at Site 1014 is further complicated by the presence of two magnetic minerals, which are locked in at different depths below the sediment/water interface.

The effect of a steep vertical overprint on the VGP path of the B–M transition at Site 1014 is illustrated in Figure 10. Because of the high positive inclinations, the northern VGPs do not reach the north rotation pole and remain close to the site. The southern VGPs exhibit the same behavior in the opposite direction because of flattening of negative inclinations.

It is difficult to exactly quantify the direction and intensity of the magnetization overprint in the x-, y-, or z-direction. Instead, we add or subtract a small component of magnetization to the measured NRM_{20mT} intensity and investigate the change in the resulting direction of magnetization. For a modification of the VGP path during the

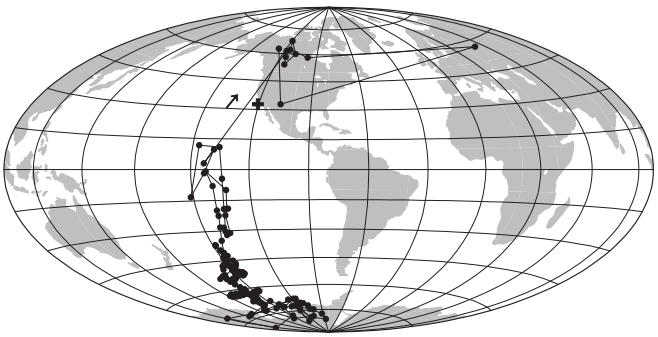

Figure 10. The VGP path of the B–M reversal was calculated from the characteristic remanent magnetizations at Hole 1014D in the Tanner Basin of the California Borderland. The VGPs do not reach the North and South geographic Poles, probably because of the drilling-induced overprint. Directional data of the ChRMs are plotted in Figure 9.

upper Jaramillo transition from Site 1020, the u-channel measurements were taken at a demagnetization step of 20 mT because many transitional VGPs are available from that reversal. If sediments are contaminated by a coring-induced overprint, the size of this overprint depends on the concentration of magnetic particles in the sediment. In the following calculations, the remanent magnetizations that were added to each u-channel measurement were proportional to the intensity of ARM. It is assumed that the intensity of the drilling remanence is proportional to the ARM, which is a measure for the amount of magnetic particles. The intensities of NRM_{20mT}, 1% of ARM and the

ratio of 0.01·ARM/NRM_{20mT}, are shown in Figure 11 for the upper Jaramillo transition. The ratio of 0.01·ARM/NRM_{20mT} varies around 0.05–0.10 for samples before and after the transition and increases to 0.4 for transitional samples. These varying amounts of 0.01·ARM are subtracted or added to the NRM_{20mT} intensities.

The VGP path is plotted in Figure 12A for the upper Jaramillo transition from u-channel measurements at a demagnetization step of 20 mT. There is a large similarity between the VGP path calculated from the ChRM directions of the u-channels (Fig. 4) and this NRM_{20mT} record (Fig. 12A). A shift of the VGP path occurs when 1% of the ARM intensity is added to the x-component of the NRM after AF demagnetization at 20 mT (NRM_{20mT}). The model calculations were conducted after correcting the declination to 0° for normal directions and to 180º for inverse directions, so that the x-axis points north. The positive z-direction points downward along the core. After adding 1% of ARM to the x-axis, the transitional VGPs move westward, and the VGPs in the Northern and Southern Hemispheres move to higher latitudes. The westward motion of the transitional VGPs becomes even larger when 2% of the ARM intensity is added to the x-component of NRM_{20mT} (Fig. 12C). This example shows that an incompletely removed radial overprint could strongly affect the VGP path during the field reversal. In addition to a radial overprint, a steep vertical overprint is frequently observed. In Figure 13 we see a combination of 1% of ARM subtracted from the x-direction and 1% of ARM (Fig. 13A), 2% of ARM (Fig. 13B), and 3% of ARM (Fig. 13C) subtracted from the z-direction. The transitional VGPs now move eastward with increasing overprint compared with the original track (Fig. 12A), and the VGPs in the Southern Hemisphere tend to lie closer to the geographic South Pole. These effects become more pronounced as we increase the overprint from Figure 13A through 13C. These simulations of synthetic overprints demonstrate that a CIM that cannot be fully removed may affect the VGP path considerably.

CONCLUSIONS

1. The characteristic remanent magnetization directions from u-channel measurements and single samples at Site 1020 are well defined before and after the magnetic reversals. The determination of ChRMs for transitional samples is more difficult because of their low intensities and the badly defined primary magnetization directions. The negative inclinations at the northern Site 1020 are slightly shallower than the value expected at this latitude for an axial geocentric dipole field. This suggests an unremoved coring-induced overprint whose coercivity spectrum overlaps with the coercivities of the ChRM. The Brunhes–Matuyama transition at the southern Site 1014 shows shallow negative and steep positive inclinations.

2. The VGP paths for the u-channel measurements and the discrete samples from the upper Jaramillo transition at Site 1020 are roughly similar. The VGPs from the u-channels track across the Pacific Ocean, whereas the only transitional VGP from the discrete samples lies over the Gulf of Mexico. The B–M reversal at Site 1020 shows differences between the u-channel measurements and the discrete sample results, so the interpretation of the transitional VGPs must be handled with caution. The effect of the drilling-induced overprint on the VGPs at Site 1020 can be seen in both records (Figs. 4, 6). In future studies, thermal demagnetization should be tried if AF treatment fails to remove the hard drilling remanence.

3. Variations in grain size and composition of magnetic particles along the core are small at Site 1020.

4. The Brunhes–Matuyama transition at Site 1014 in the Tanner Basin demonstrates convincingly the persistent nature of the drilling-

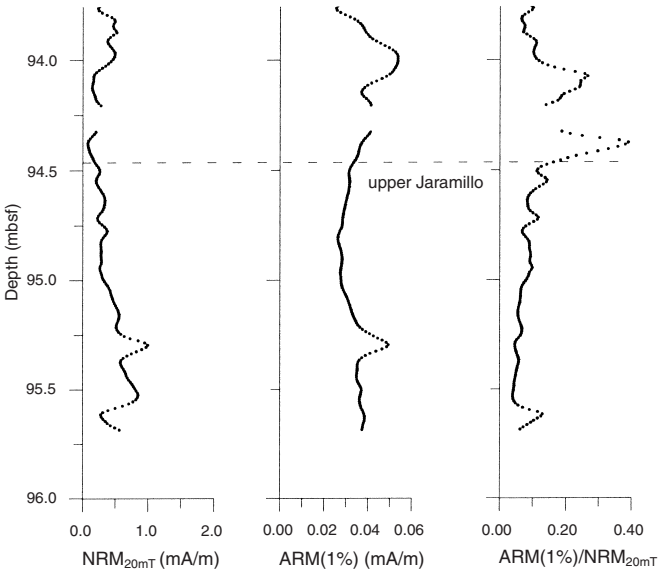

Figure 11. Plot of natural remanent magnetization $(NRM)_{20mT}$ intensity, 1% of anhysteretic remanent magnetization (ARM), and the ratio of these values vs. depth for the upper Jaramillo at Site 1020. The region of the transition is marked with a dashed line. For the transitional samples, the ratio 0.01·ARM/NRM_{20mT} increases to 0.4.

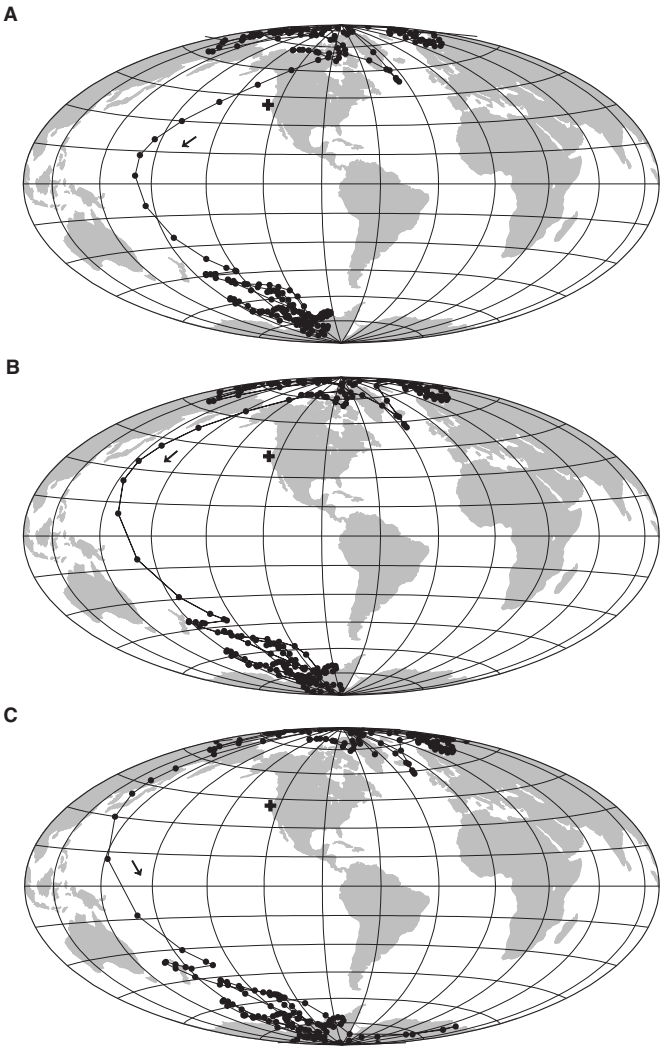

Figure 12. **A.** VGP path of the upper Jaramillo transition at the demagnetization step of 20 mT from u-channel measurements. The influence of a radial overprint in the x-direction was modeled by adding a remanence that is proportional to 1% or 2% of ARM. **B.** Positive x-component of NRM_{20mT} + 0.01·ARM. **C.** Positive x-component of NRM_{20mT} + 0.02·ARM.

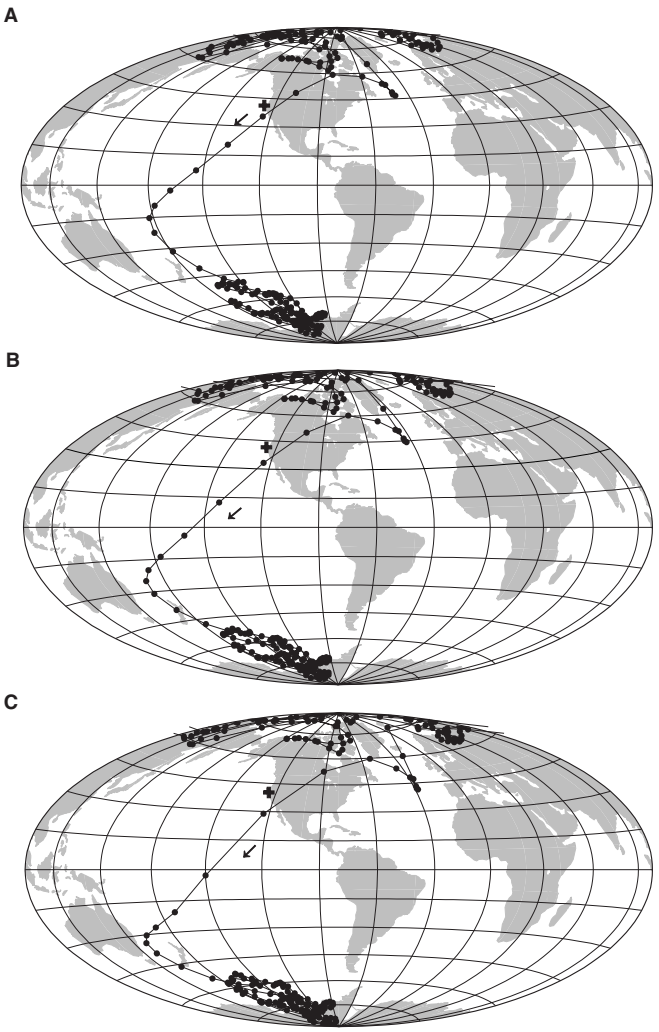

Figure 13. These calculations model the simultaneous effects of vertical and radial overprints on the NRM. **A.** The x-component of $NRM_{20mT} - 0.01 \cdot ARM$; z-component of $NRM_{20mT} - 0.01 \cdot ARM$ intensity. **B.** The x-component of $NRM_{20mT} - 0.01 \cdot ARM$; z-component of $NRM_{20mT} - 0.02 \cdot ARM$. **C.** The x-component of $NRM_{20mT} - 0.01 \cdot ARM$; z-component of $NRM_{20mT} - 0.03 \cdot ARM$.

induced overprint. In that case the VGPs do not reach the geographic North or South Pole. As a result of the two magnetic minerals and the NRM intensity drop in the sediments of Site 1014, the directional record of these sediments should only be regarded as an illustration of a persistent coring-induced magnetization.

5. Because of the hard coring-induced remanence components, we do not consider any of the transitional records from this study suitable for extracting details about the geomagnetic field.

6. Model calculations for the VGP paths of the upper Jaramillo transition show that incompletely removed radial and vertical overprints can strongly affect the track of the VGPs. The antipodality of normal and inverse directions can be improved by subtracting a radial and vertical component of magnetization. Previously measured records from ODP cores must be investigated for the possible presence of coring-induced overprints.

ACKNOWLEDGMENTS

We thank Drs. B. Herr, M. Fuller, N. Petersen, and H. Soffel for constructive criticism and fruitful discussions. We are grateful to Dr. K.L. Verosub for making available his laboratory and cryogenic magnetometer for the u-channel measurements. Comments by Drs. G. Acton, C. Richter, and J.S. Stoner on the manuscript were appreciated. This research was supported by the Grants He 1814/8-2 and 8-3 from the Deutsche Forschungsgemeinschaft.

REFERENCES

Bloemendal, J., King, J.W., Hall, F.R., and Doh, S.-J., 1992. Rock magnetism of late Neogene and Pleistocene deep-sea sediments: relationship to sediment source, diagenetic processes, and sediment lithology. *J. Geophys. Res.,* 97:4361–4375.

Cande, S.C., and Kent, D.V., 1995. Revised calibration of the geomagnetic polarity timescale for the Late Cretaceous and Cenozoic. *J. Geophys. Res.,* 100:6093–6095.

Clement, B.M., 1991. Geographical distribution of transitional VGPs: evidence for non-zonal equatorial symmetry during the Matuyama-Brunhes geomagnetic reversal. *Earth Planet. Sci. Lett.,* 104:48–58.

Day, R., Fuller, M., and Schmidt, V.A., 1977. Hysteresis properties of titanomagnetites: grain-size and compositional dependence. *Phys. Earth Planet. Inter.,* 13:260–267.

Fuller, M., Hastedt, M., and Herr, B., 1998. Coring-induced magnetization of recovered sediment. *In* Weaver, P.P.E., Schmincke, H.-U., Firth, J.V., and Duffield, W. (Eds.), *Proc. ODP, Sci. Results,* 157: College Station, TX (Ocean Drilling Program), 47–56.

Herr, B., Fuller, M., Haag, M., and Heider, F., 1998. Influence of drilling on two records of the Matuyama/Brunhes polarity transition in marine sediment cores near Gran Canaria. *In* Weaver, P.P.E., Schmincke, H.-U., Firth, J.V., and Duffield, W. (Eds.), *Proc. ODP, Sci. Results,* 157: College Station, TX (Ocean Drilling Program), 57–69.

Hoffman, K.A., 1992. Dipolar reversal states of the geomagnetic field and core-mantle dynamics. *Nature,* 359:789–794.

Laj, C., Mazaud, A., Fuller, M., Weeks, R., and Herrero-Bervera, E., 1991. Lateral variations at the core-mantle boundary revealed by geomagnetic reversal paths? *Nature,* 351:447.

Langereis, C.G., van Hoof, A.A.M., and Rochette, P., 1992. Longitudinal confinement of geomagnetic reversal paths: sedimentary artifact or true field behavior. *Nature,* 358:226–229.

Love, J.J., 1998. Paleomagnetic volcanic data and geometric regularity of reversals and excursions. *J. Geophys. Res.,* 103:12435–12452.

Lyle, M., Koizumi, I., Richter, C., et al., 1997. *Proc. ODP, Init. Repts.,* 167: College Station, TX (Ocean Drilling Program).

McFadden, P.L., Barton, C.E., and Merrill, R.T., 1993. Do virtual geomagnetic poles follow preferred paths during geomagnetic reversals? *Nature,* 361:342–344.

Prévot, M., and Camps, P., 1993. Absence of preferred longitude sectors for poles from volcanic records of geomagnetic reversals. *Nature,* 366:53–57.

Roberts, A.P., Stoner, J.S., and Richter, C., 1996. Coring induced magnetic overprints and limitations of the long-core paleomagnetic measurements technique: some observations from Leg 160, eastern Mediterranean Sea. *In* Emeis, K.-C., Robertson, A.H.F., Richter, C., et al., *Proc. ODP, Init. Repts.,* 160: College Station, TX (Ocean Drilling Program), 497–505.

Tauxe, L., 1993. Sedimentary records of relative paleointensity of the geomagnetic field: theory and practice. *Rev. Geophys.,* 31:319–354.

Weeks, R.J., Laj, C., Endignoux, L., Fuller, M.D., Roberts, A.P., Manganne, R., Blanchard, E., and Goree, W., 1993. Improvements in long-core measurement techniques: applications in palaeomagnetism and palaeoceanography. *Geophys. J. Int.,* 114:651–662.

Date of initial receipt: 18 November 1998
Date of acceptance: 30 April 1999
Ms 167SR-208